Comments on the optical lineshape function: Application to transient hole-burned spectra of bacterial reaction centers

Mike Reppert, Adam Kell, Thomas Pruitt, and Ryszard Jankowiak

Citation: The Journal of Chemical Physics **142**, 094111 (2015); doi: 10.1063/1.4913685

View online: http://dx.doi.org/10.1063/1.4913685

View Table of Contents: http://scitation.aip.org/content/aip/journal/jcp/142/9?ver=pdfcov

Published by the AIP Publishing

Comments on the optical lineshape function: Application to transient hole-burned spectra of bacterial reaction centers

Mike Reppert,[1,a)] Adam Kell,[1] Thomas Pruitt,[1,b)] and Ryszard Jankowiak[1,2,c)]
[1]*Department of Chemistry, Kansas State University, Manhattan, Kansas 66506, USA*
[2]*Department of Physics, Kansas State University, Manhattan, Kansas 66506, USA*

(Received 12 January 2015; accepted 16 February 2015; published online 4 March 2015)

The vibrational spectral density is an important physical parameter needed to describe both linear and non-linear spectra of multi-chromophore systems such as photosynthetic complexes. Low-temperature techniques such as hole burning (HB) and fluorescence line narrowing are commonly used to extract the spectral density for a given electronic transition from experimental data. We report here that the lineshape function formula reported by Hayes *et al.* [J. Phys. Chem. **98**, 7337 (1994)] in the mean-phonon approximation and frequently applied to analyzing HB data contains inconsistencies in notation, leading to essentially incorrect expressions in cases of moderate and strong electron-phonon (el-ph) coupling strengths. A corrected lineshape function $L(\omega)$ is given that retains the computational and intuitive advantages of the expression of Hayes *et al.* [J. Phys. Chem. **98**, 7337 (1994)]. Although the corrected lineshape function could be used in modeling studies of various optical spectra, we suggest that it is better to calculate the lineshape function numerically, without introducing the mean-phonon approximation. New theoretical fits of the P870 and P960 absorption bands and frequency-dependent resonant HB spectra of *Rb. sphaeroides* and *Rps. viridis* reaction centers are provided as examples to demonstrate the importance of correct lineshape expressions. Comparison with the previously determined el-ph coupling parameters [Johnson *et al.*, J. Phys. Chem. **94**, 5849 (1990); Lyle *et al.*, *ibid.* **97**, 6924 (1993); Reddy *et al.*, *ibid.* **97**, 6934 (1993)] is also provided. The new fits lead to modified el-ph coupling strengths and different frequencies of the special pair marker mode, ω_{sp}, for *Rb. sphaeroides* that could be used in the future for more advanced calculations of absorption and HB spectra obtained for various bacterial reaction centers. © *2015 AIP Publishing LLC.* [http://dx.doi.org/10.1063/1.4913685]

I. INTRODUCTION

The rapid growth of laser-based spectroscopies over the last several decades has enabled important developments in almost every field of the physical sciences, from quantum optics to the single-molecule study of biological molecules. In biophysics, in particular, newly developed spectroscopies have greatly increased our ability to probe the structure, dynamics, and interactions of biomacromolecules and the ligands they bind.

The utility of laser-based techniques is perhaps nowhere as evident as in the study of the chlorophyll-protein complexes involved in photosynthetic energy harvesting and transduction. In characterizing these complex systems, complementary techniques have been developed for different purposes. Frequency-domain methods such as hole-burning (HB) and fluorescence line narrowing (FLN) take advantage of the narrow lineshapes and energetic stability offered by low-temperatures (4–77 K) to characterize excitonic interactions and site-specific spectroscopic characteristics which are often blurred by thermal motion at higher temperatures.[1,2] Room temperature time-domain measurements, in contrast, while substantially complicated by the broad, relatively featureless, spectral properties of higher temperature systems, offer the essential advantage of allowing for the characterization of samples not only under biological conditions *in vitro* but even *in vivo* in living bacterial cells.[3–5]

To build a complete picture of any physical system, one must of course be able to compare the results obtained using different methods. In connecting time- and frequency-domain spectroscopic measurements, perhaps the most important point of comparison is the *phonon spectral density*, $J(\omega)$, a frequency-domain profile which describes how strongly a given electronic transition couples to the vibrational motions of a pigment or its environment.[6] In the frequency domain, the spectral density determines transition line shapes for both linear absorption experiments and non-linear multi-dimensional methods. In the time domain, the spectral density determines the frequency-correlation function, which in turn defines the non-linear system response.[6] Low-temperature, frequency-domain methods such as HB and FLN, which provide particularly convenient access to the spectral density, may thus be used in conjunction with time-domain measurements and simulations to provide a holistic characterization of both experimental results and theoretical predictions.

[a)]Permanent address: Department of Chemistry, The University of Chicago, Chicago, Illinois 60637, USA.
[b)]Permanent address: Department of Chemistry, The Ohio State University, Columbus, Ohio 43210, USA.
[c)]Author to whom correspondence should be addressed. Electronic mail: ryszard@ksu.edu

In this light, the importance of the accurate evaluation of the spectral density from experimental data is evident. For this purpose, HB spectra in a variety of systems (including various photosynthetic complexes) have often been modeled (e.g., Refs. 7–18) by the temperature-dependent lineshape formulas developed by Hayes *et al.*[19] These formulas provide analytical expressions for HB spectra in terms of an assumed spectral density, allowing for the extraction of $J(\omega)$ by fitting experimental spectra against calculated lineshapes.[19,20] It has recently come to our attention while modeling transient HB spectra in a bacterial Zn-reaction center (Zn-RC) and its mutant (Zn-β-RC)[21] that the lineshape function formulas in the mean-phonon approximation given in Ref. 19 contain inconsistencies in notation, leading in some cases (i.e., for moderate and strong electron-phonon (el-ph) coupling strengths) to incorrect expressions. While for simple systems these inconsistencies are insignificant, for cases of strong el-ph coupling like those observed in bacterial RCs[20,22] (where multiple phonon transitions are involved) they lead to significant errors.[21] To clarify the situation, in this work, we derive corrected lineshape formulas under the same assumptions as made by Hayes *et al.*,[19] while focusing on the various approximations appearing in these expressions and their physical significance. For routine analysis of HB spectra, however, we suggest that the lineshape should generally be evaluated numerically without the introduction of the mean-phonon approximation.

II. DERIVATION OF LINESHAPE FORMULAS

We begin with the well-known formula describing the absorption and fluorescence lineshape functions[23]

$$L_{A/F}(\omega) = e^{-S(T)} \int_{-\infty}^{\infty} e^{\pm i(\omega-\Omega_0)t + G(t;T)} dt, \tag{1}$$

where Ω_0 is the zero-phonon line (ZPL) frequency, and $n(\omega;T) = \frac{1}{e^{\hbar\omega/kT}-1}$ is the thermal occupation number at temperature T and frequency ω. $J(\omega)$ is the spectral density referred to in the Introduction. $G(t;T)$ is the time-domain lineshape function[23]

$$G(t;T) = \int_{-\infty}^{\infty} e^{-i\omega t} \left[(1 + n(\omega;T)) J(\omega) + n(-\omega;T) J(-\omega) \right] d\omega, \tag{2}$$

and $S(T) = G(0,T)$ is a temperature-dependent effective Huang-Rhys factor. In the exponent of Eq. (1), "+" refers to absorption (L_A), while "–" refers to fluorescence (L_F). By definition, $L_A(\omega - \Omega_0) = L_F(\Omega_0 - \omega)$; i.e., the two functions are mirror images of each other around Ω_0.

Although the above lineshape functions are well-known and easily computed numerically, they are not very physically transparent. Therefore, a more intuitive formula was obtained by expanding the exponent inside the integral as an infinite sum.[20] Physically, this expansion allows us to divide the lineshape into "R-phonon" profiles, i.e., separate terms corresponding to transitions involving the creation or annihilation of R phonon excitations. For arbitrary temperatures, Eq. (1) can then be written as[20,22]

$$L_{A/F}(\omega) = \underbrace{e^{-S(T)} l_0(\omega - \Omega_0)}_{ZPL} + \underbrace{\sum_{R=1}^{\infty} S(T)^R \frac{e^{-S(T)}}{R!} l_R(\pm\omega - R\omega_m - \Omega_0)}_{PSB}, \tag{3}$$

where $+\omega$ and $-\omega$ correspond to absorption $L_A(\omega)$ and fluorescence $L_F(\omega)$, respectively.

The first term in this expression represents the Lorentzian ZPL $l_0(\omega - \Omega_0)$ which peaks at Ω_0 and possesses a homogeneous width Γ_{hom}. The second term is the phonon sideband (PSB), consisting of a sum over all R-phonon transitions. The constant ω_m is the peak (or mean) phonon frequency, i.e., the peak frequency of $J(\omega)$. At low temperatures, each R-phonon spectrum $l_R(\pm\omega - R\omega_m - \Omega_0)$ peaks at a frequency roughly $R\omega_m$ higher (absorption) or lower (fluorescence) in frequency than the ZPL, underscoring the physical significance of these profiles as corresponding to the creation or annihilation of R phonon excitations.

More explicitly, the *one-phonon profile* $l_1(\omega)$ is the Fourier transform of $G(t;T)$, or in the frequency domain,

$$l_1(\omega) = \frac{1}{S(T)} \left[(1 + n(\omega + \omega_m;T)) J(\omega + \omega_m) + n(-\omega - \omega_m;T) J(-\omega - \omega_m) \right]. \tag{4}$$

Effectively, the one-phonon profile is a temperature-weighted spectral density function. For comparison with the work of Hayes *et al.*,[19] we define it here to be normalized and shifted by the mean phonon frequency ω_m so that at low temperatures ($n(\omega + \omega_m;T) \approx 0$), its peak occurs at zero frequency; this zero-frequency peak in $l_1(\omega)$ gives rise to the one-phonon Stokes portion of the PSB near $\Omega_0 + \omega_m$ in the absorption spectrum via the $l_R(\omega - \omega_m - \Omega_0)$ term in our expansion. At high temperatures, the $n(-\omega - \omega_m;T)$ term becomes significant and gives rise to an additional anti-Stokes peak near $\Omega_0 - \omega_m$ in the absorption spectrum. For $R > 1$, $l_R(\omega)$ is the similarly shifted and normalized Fourier transform of $G(t;T)^R$ or, equivalently, the $(R-1)$-fold convolution of $l_1(\omega)$ with itself. The shape of each $l_R(\omega)$ is thus equivalently determined by either $G(t;T)$ or $l_1(\omega)$.

Before we proceed with our derivation, it is worth pausing to comment on the shape of the R-phonon profile $l_R(\omega)$. At low temperatures, the one-phonon profile $l_1(\omega)$ closely resembles the spectral density $J(\omega)$. Guided by the experimental work in Refs. 8–10 and references given therein, the spectral density $J(\omega)$ is often assumed to be asymmetric with a Gaussian shape at its low-energy wing and a Lorentzian shape at its high-energy wing; the profile then has a peak frequency of ω_m and a width of $\Gamma = \Gamma_G/2 + \Gamma_L/2$. In their modeling work, Hayes *et al.*[19] extended this functional form to calculate the R-phonon profile—properly an $(R-1)$-fold convolution—as a Gaussian of width $\sqrt{R}\Gamma_G$ on the low-frequency side and a Lorentzian of width $R\Gamma_L$ on the high-frequency side (see Eqs. (15a) and (15b) in Ref. 19, along with many later works[7–18]). Although such a profile does provide a reasonable approximation to the true form of $l_R(\omega)$ at low temperatures when the Gaussian and Lorentzian components have similar widths, the approximation breaks down quite seriously when Γ_G is much different from $\sqrt{R}\Gamma_L$ (see below). As many-fold convolutions

are trivial on a modern desktop computer, the numerical convolution of the one-phonon profile is much preferable to this approximate form.

Returning to Eq. (3), we next note that, for relatively narrow one-phonon profiles, an additional simplifying approximation can be made, where in Eqs. (2) and (4) the frequency dependent function $n(\omega)$ is replaced by an average value $\bar{n} = n(\omega_{\mathrm{m}})$. In this case, the expression for $l_1(\omega)$ can be split up into two terms, one proportional to $J(\omega + \omega_{\mathrm{m}})$ and the other to $J(-\omega - \omega_{\mathrm{m}})$. The sum over R then splits into two sums, one numbering the total number, R, of phonons involved in the transition and the other, $P = 0, \ldots, R$, indicating how many phonons are annihilated (as opposed to created) during the transition

$$L_{A/F}(\omega) \approx e^{-S(2\bar{n}+1)} \sum_{R=0}^{\infty} \sum_{P=0}^{R} \frac{[S(\bar{n}+1)]^{R-P}[S\bar{n}]^{P}}{(R-P)!P!} \times l_{R,P}(\pm\omega - \Omega_0 + (R-2P)\omega_m). \quad (5)$$

For example, with three phonons created ($R = 3$, $P = 0$), the PSB peaks at $\Omega_0 + 3\omega_{\mathrm{m}}$. However, if two of the phonons are annihilated ($R = 3, P = 2$), the corresponding transition peaks at $\Omega_0 - \omega_{\mathrm{m}}$ and gives rise to the anti-Stokes part of the PSB.

The derivation of this expression follows almost identically to that employed by Hayes *et al.* (Eqs. (4)–(14) of Ref. 19). Briefly, the time-domain lineshape function $G(t;T)$ is divided into creation and annihilation terms $G_+(t;T)$ and $G_-(t;T)$:

$$G_+(t;T) = (1+\bar{n}) \int_{-\infty}^{\infty} e^{-i\omega t} J(\omega)\, d\omega, \quad (6a)$$

$$G_-(t;T) = \bar{n} \int_{-\infty}^{\infty} e^{-i\omega t} J(-\omega)\, d\omega. \quad (6b)$$

After expanding the exponent in Eq. (1) in a Taylor series, the binomial formula is used to group together terms involving a total of R factors of either G_+ or G_-, i.e., terms proportional to $G_+^{R-P}G_-^{P}$ with $P = 0, \ldots, R$. Fourier transforming these terms back to the frequency domain gives the lineshapes $l_{\mathrm{R,P}}(\omega)$ which together constitute the total absorption or fluorescence spectrum.

Within the mean-phonon approximation, Eq. (5) is correct as written and is in agreement with Eq. (17) of Hayes *et al.*[19] On closer inspection, however, two important errors may be identified in the expressions of Hayes *et al.*[19]

The first error arises in specifying the form of the individual profiles $l_{\mathrm{R,P}}(\omega)$. Correctly, these terms arise as Fourier transforms of the time-domain products $G_+^{R-P}G_-^{P}$. In the frequency domain, they thus correspond to the convolution of the Fourier transforms of G_+^{R-P} and G_-^{P}. The profile $l_{\mathrm{R,P}}(\omega)$ thus corresponds to an $(R-1)$-fold convolution involving $R-P$ occurrences of $J(\omega)$ and P occurrences of $J(-\omega)$. All profiles may, in this case, be obtained by setting $l_{1,0}(\omega)$ equal to $J(\omega)$ and convolving this function with itself $R-P-1$ times and with its reflection $P-1$ times.

In contrast, Hayes *et al.*[19] obtained the multi-phonon profiles $l_{\mathrm{R,P}}(\omega)$ from the one-phonon profile by convolving $l_{1,0}(\omega)$ with itself $|R-2P| - 1$ times. This approach is qualitatively incorrect: whereas the width of the $l_{\mathrm{R,P}}(\omega)$ should be roughly proportional to R (the total number of convolutions), the expressions of Hayes *et al.*[19] indicate a width proportional to $|R-2P|$. That this result is physically incorrect may be seen by considering the case $R = 2P$, i.e., to a transition involving an equal number of creation and annihilation events. The expressions of Hayes *et al.*,[19] in this case, call for an unphysical, infinitely sharp phonon profile; the correct lineshape has a width roughly proportional to R, indicating the convolved distribution of phonon frequencies which may be involved in each creation or annihilation event.

The second serious discrepancy introduced by Hayes *et al.*[19] comes in their description of the Franck-Condon factors and absorption spectra of systems with discrete spectral densities, i.e., under the assumption that $J(\omega)$ may be written as a discrete sum of delta functions

$$J(\omega) = \sum_{k=1}^{N} S_k \delta(\omega - \omega_k). \quad (7)$$

Such a density might be used, for example, to model the absorption due to a small number of high-frequency local vibrational modes of a single pigment. Following a derivation parallel to that used to obtain Eq. (5), one may in this case write the absorption lineshape function as

$$L(\omega) = e^{-\sum_{k=1}^{N} S_k(2n_k+1)} \times \sum_{R_1=0}^{\infty} \sum_{P_1=0}^{R_1} \cdots \sum_{R_N=0}^{\infty} \sum_{P_N=0}^{R_N} \prod_{k=1}^{N} \frac{[S_k(n_k+1)]^{R_k-P_k}[S_k n_k]^{P_k}}{(R_k-P_k)!P_k!} \times \delta\left(\omega - \sum_{k=1}^{N}(R_k - 2P_k)\omega_k\right). \quad (8)$$

In this case, the absorption spectrum consists of a discrete sum of peaks occurring at any integer combination of the peak frequencies ω_{k} appearing in the spectral density. This expression may be obtained directly by evaluating the Fourier transform in Eq. (12) of Hayes *et al.*[19] In that work, however, an error or inconsistency in notation occurs in passing from Eq. (12) to Eq. (13), leading to an incorrect lineshape function reading

$$L(\omega) = e^{-\sum_{k=1}^{N} S_k(2\bar{n}_k+1)} \times \prod_{k=1}^{N} \sum_{\mathrm{R}=0}^{\infty} \sum_{P=0}^{R} \frac{[S_k(\bar{n}_k+1)]^{R-P}[S_k\bar{n}_k]^{P}}{(R-P)!P!} \times \delta\left(\frac{-E}{\hbar} - \sum_k \omega_k(R-2P)\right). \quad (9)$$

(Hayes *et al.*[19] refer to this as a frequency-dependent Franck-Condon factor; it is equivalent, however, to the lineshape function for a discrete spectral density.) In this expression, the index k enumerates a product, rather than a series of sums, over the individual phonon modes. Apparently, the product over k in the time-domain expression was incorrectly carried over to the frequency domain, rather than being converted to a convolution.

Again, Eq. (9) is easily seen to be physically incorrect, carrying an improper dependence on the number of phonons involved in the transition: due to the appearance of only a single pair of indices, R and P, to count phonon numbers, all phonon peaks are forced to appear at multiples of the summed frequency $\omega_1 + \omega_2 + \omega_3 + \ldots + \omega_N$, with no peaks occurring at the fundamental frequencies $\omega_1, \omega_2, \ldots, \omega_N$. In the correct expression, Eq. (8), the single pair of sums over R and P is

TABLE I. Electron-phonon coupling parameters for *Rb. sphaeroides*, *Rps. viridis*, and Zn-RC. All values in units of cm^{-1} except S (dimensionless).

	ω_{ph}	Γ_G^{ph}	Γ_L^{ph}	S_{ph}	ω_{sp}	Γ_L^{sp}	S_{sp}	$S_{sp}\omega_{sp}$	S_{tot}	Γ_{hom}	ω_{SDF}	Γ_{inh}
Original *Rb. sphaeroides*[a]	30	30	55	1.8	115	50	1.5	173	3.3	5.75	10 992	150
Revised *Rb. sphaeroides*[b]	28	25	30	2.1	125	30	1.3	163	3.4	5.75	10 982	140
Original *Rps. viridis*[c]	30	30	55	2.2	145	25	1.1	160	3.3	**	**	140
Revised *Rps. viridis*[b]	25	20	30	2.0	145	30	1.1	160	3.1	5.75	9 785	140
Zn-RC *Rb. sphaeroides*[d]	30	25	25	3.6	130	25	1.0	130	4.6	5	11 120	110

[a]Reference 8.
[b]This work.
[c]Reference 9.
[d]Reference 21.

replaced by a pair of sums for each of the N phonon modes, allowing for both creation and annihilation of all phonons in any combination.

We emphasize again that the assumptions used to derive Eq. (8) are identical to those for Eq. (9) but that Eq. (9) is in error. Note also that Eq. (9) cannot be corrected by replacing the product with a single sum over k (as has sometimes been done in the literature[19,24]) because in that case one still has all terms peaking at multiples of $\omega_1 + \omega_2 + \omega_3 + \ldots + \omega_N$. Indeed, the product gives the correct area factors for the peaks, but their position is wrong. The product should instead be replaced by the convolution over k of the lineshape functions (in this case, simply a sum of delta functions).

Finally, we should note that for modeling HB spectra, Hayes *et al.*[19] combine their expressions (corresponding to Eqs. (5) and (9) in this work) to produce a "hybrid" absorption expression involving finite-width profiles $l_{R,P}(\pm\omega - \Omega_0 + (R - 2P)\omega_m)$ with Franck-Condon factors described (incorrectly) by Eq. (9). Such an expression might be used to model a system with a spectral density of the form

$$J(\omega) = \sum\nolimits_k S_k J_k(\omega - \omega_k), \tag{10}$$

where each $J_k(\omega)$ is a normalized profile corresponding to a phonon mode with frequency ω_k. In the case that each of the profiles $J_k(\omega)$ are identical, the absorption lineshape can be obtained directly from Eq. (9) by replacing the delta function $\delta(\omega)$ with the correctly convolved lineshape $l_{R,P}(\omega)$ described earlier in our discussion. In the case that the profiles $J_k(\omega)$ are different from one another, a correct expression for the corresponding lineshape $l_{R_1,P_1,\ldots,R_N,P_N}(\omega)$ may be derived in terms of the many-fold convolution of the various profiles and their reflections. The expressions, however, are quite bulky and of limited utility for more than one or two modes. Unless the individual contributions of these terms are specifically required for a given analysis, it seems much more feasible to calculate the absorption spectrum directly—without imposing the mean-phonon approximation—using the exact expressions of either Eq. (1) or Eq. (3).

III. APPLICATION TO BACTERIAL REACTION CENTERS

A. Calculation of HB spectra

Finally, in order to emphasize the importance of correctly evaluating the absorption lineshape function, we apply the expressions above to the description of various P870 and P960 absorption bands and resonant (transient) HB spectra obtained for bacterial RCs of *Rb. sphaeroides* and *Rps. viridis*. Transient holes (T ~ 5 K) upon selective laser excitation within the P870 and/or P960 absorption bands are due to charge separation and measured during the $P^+Q_A^-$ charge separated state. Note that Eq. (1) can be used for arbitrary PSB shapes, and the direct numerical approach (*vide infra*) can be used in modeling of HB spectra. Very recently, we provided a critical assessment of typical phonon spectral densities, $J(\omega)$, used to describe linear and non-linear optical spectra in photosynthetic complexes;[25] see also Refs. 26 and 27 for discussion on various functions used for spectral densities. $J(\omega)$ describes the frequency-dependent coupling of the system to the bath and is an important component in calculations of optical spectra (including HB spectra) and excitation energy transfer times. Based on the shape of experimental $J(\omega)$ obtained for several photosynthetic complexes, we showed that many $J(\omega)$ (especially the Drude-Lorentz/constant damping Brownian oscillator) display qualitatively wrong behavior when compared to experiment.[25] Therefore, we proposed that a lognormal distribution, which exhibits desired attributes for a physically meaningful phonon $J(\omega)$, should be used to fit experimental data, in contrast to several commonly used spectral densities which exhibit low frequency behavior in qualitative disagreement with experiment. We also demonstrated that the half-Gaussian-half-Lorentzian (G–L) $J(\omega)$ used in modeling of HB spectra should be replaced with the lognormal function, which provides a more physically realistic fit of the high-energy side of experimental spectral densities (e.g., FMO and CP29).[25] The absence of the long Lorentzian tail in the lognormal function (that is present in G-L $J(\omega)$) eliminates problems associated with continuously increasing reorganization energy E_λ, which is not well defined since the integral does not converge for the Lorentzian. The lognormal form also solves problems with the zero frequency behavior of the constant damping Brownian oscillator $J(\omega)$, which contradicts experiment.

To make a direct comparison to the previously published data, in this letter we describe the shapes of P870 and P960 absorption bands and transient HB spectra using both G-L and lognormal $J(\omega)$. We anticipate that our results will provide new insight into el-ph coupling parameters for *Rb. sphaeroides* and *Rps. viridis* which could be used in future modeling studies using more advanced theories. We compare el-ph coupling parameters obtained previously for *Rb.* sphaeroides[8,28] and *Rps. viridis*,[9,28] using the approach of Hayes *et al.*,[19] with the parameters obtained in this work (using both G-L and

TABLE II. Electron-phonon coupling parameters for lognormal spectral densities.[a]

	ω_c	σ	S_{ph}	E_λ	ω_{sp}	Γ_L^{sp}	S_{sp}	$S_{sp}\omega_{sp}$	S_{tot}	Γ_{hom}	ω_{SDF}	Γ_{inh}
Rb. sphaeroides	35	0.47	1.7	82	125	30	1.5	163	3.2	5.75	10 975	150
Rps. viridis	29	0.40	1.9	60	145	30	1.2	174	3.1	5.75	9 785	140

[a]All values in units of cm^{-1} except S and σ (dimensionless).

lognormal spectral densities). We hasten to add that in our approach, we properly account for mixed transitions (i.e., multi-phonon transitions involving creation or annihilation of phonons), as discussed above. It has been shown[20,22] that in the low temperature limit, the HB spectrum is defined by $\Delta A = A(\Omega,t) - A(\Omega,0)$, where $A(\Omega,0)$ is the pre-burn absorption spectrum, and

$$A(\Omega,t) = \int L_A(\omega-\Omega)\,N(\omega)\,e^{-P\sigma\phi L_A(\omega_B-\omega)t}\,d\omega \qquad (11)$$

is the post-burn absorption spectrum. In Eq. (11), ω_B is the burn/excitation frequency, P is the photon flux, t is the burn time, $N(\omega)$ is the pre-burn site distribution function (SDF), describing the probabilities of encountering different zero-phonon transition frequencies, and $L_A(\omega)$ is the single site absorption profile. In the low-fluence limit, the exponent in Eq. (11) can be expanded in a Taylor series to obtain

$$A(\Omega,t) \approx A(\Omega,0) - P\sigma\phi t \times \int L_A(\omega-\Omega)\,N(\omega)\,L_A(\omega_B-\omega)\,d\omega. \qquad (12)$$

For the calculations presented in this work, the absorption lineshape function $L_A(\omega_B-\omega)$ was calculated using Eq. (3). As described above, the higher-order profiles $l_R(\omega;T)$ were obtained by numerical convolution of the one-phonon profile with itself ($R-1$ times) and with the ZPL; the sum was truncated after a number of terms sufficient to account for 99.99% of the total intensity of the PSB. Finally, to account for lifetime broadening of the transition, the lineshape function $L_A(\omega)$ given by Eq. (3) was convolved with a Lorentzian lineshape function before evaluating Eq. (12). This approach is compared below with the mean-phonon approximation used in earlier calculations,[8,9,28] where the spectral density was split into multiple effective phonon densities and the continuous weighting factor $n(\omega;T)$ was replaced by an effective factor $n(\omega_k;T)$ evaluated at a "mean" phonon frequency ω_k near the peak of the kth phonon density; and where in place of numerical convolutions, multi-phonon transitions were described simply as increasingly broadened G-L profiles.

We suggest that the approach with a lognormal spectral density describes the phonon lineshape more accurately,[25] although to reveal the difference between our approach and that of Hayes *et al.*,[19] i.e., to compare our parameters with the previously published data,[8,9,28] we also show fits and parameters obtained with the G-L $J(\omega)$. On the basis of previous work,[8,9,28] only two profiles corresponding to peak frequencies ω_{ph} and ω_{sp} are required to simultaneously fit the P870 and P960 absorption bands and ω_B-dependent photochemical (transient) HB spectra. Consistent with earlier assignment, we refer to ω_{ph} as the mean (or rather peak) phonon frequency and ω_{sp} as the special pair marker mode.[7] Special pair marker modes are intermolecular vibrational modes localized on the special pair.[7] The lineshape for the ω_{ph} mode is described by a Gaussian (fwhm = Γ_G^{ph} cm^{-1}) and Lorentzian (fwhm = Γ_L^{ph} cm^{-1}) on the low- and high-energy sides, respectively, or by the lognormal spectral density. As suggested in Refs. 8, 9, 19, and 28 a Lorentzian lineshape (fwhm = Γ_L^{sp} cm^{-1}) is used for the ω_{sp} mode. However, in contrast to previous work, the special pair and phonon densities are combined into a single spectral density $J(\omega)$ before the evaluation of Eq. (3), taking into account mixed transitions (i.e., multi-phonon transitions involving creation or annihilation of phonons from both profiles) directly and with no additional approximations. Using numerical calculations (*vide infra*) of P870 and P960 absorption bands and resonant HB spectra, i.e., making the direct calculation of the convoluted l_R terms, new sets of parameters (Huang-Rhys factors, Γ_{inh}, $J(\omega)$ parameters, etc.) for *Rb. sphaeroides* and *Rps. viridis* have been obtained (see Tables I and II for details).

B. Single site absorption spectra for different Huang-Rhys factors

Comparison of single site absorption spectra (5 K) calculated with the method presented in Hayes *et al.*[19] and this work shows that larger deviations in calculations occur for stronger el-ph coupling (see Figure 1). The differences between these two methods are also more clearly visible for asymmetric

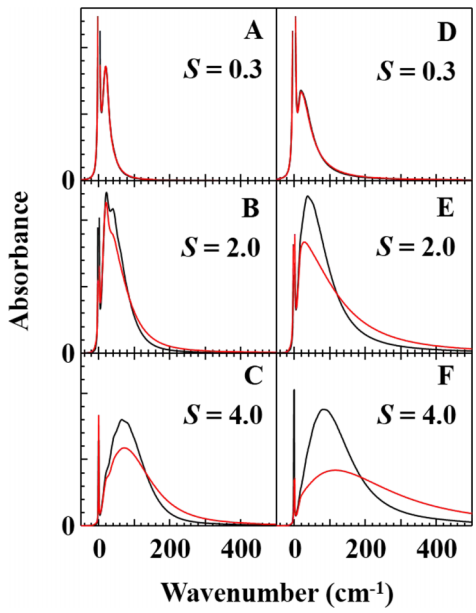

FIG. 1. Calculated single site absorption spectra (5 K) for different S values with set parameters using the method of Hayes *et al.*[19] (black curves) and this work (red curves) using a G-L shape for the spectral density. $\omega_{ph} = 20$ cm^{-1}, $\Gamma_{hom} = 1$ cm^{-1}, $\Gamma_G = 20$ cm^{-1}. $\Gamma_L = 20$ cm^{-1} for frames (a)-(c) and 60 cm^{-1} for frames (d)-(f).

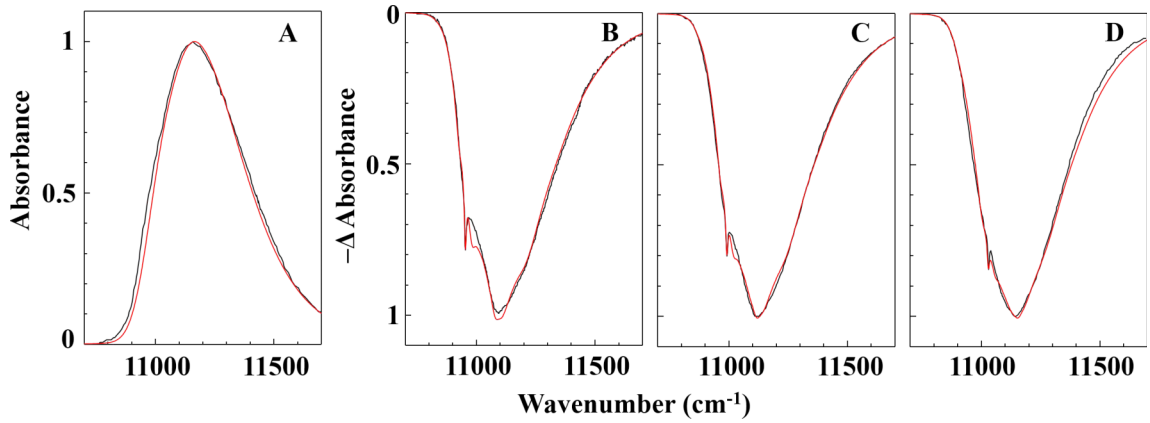

FIG. 2. Experimental data[8] (black curves) and simulated curves using a G-L $J(\omega)$ (red curves) for *Rb. sphaeroides* using the method outlined in this work. Frame (a) is the absorption spectrum for P870 while frames (b)-(d) are transient HB spectra obtained with burning frequencies of $\omega_B = 10\,953$, 10 992, and 11 030 cm^{-1}, respectively. Experimental spectra are normalized to one and calculated HB spectra are normalized to the experimental ZPH depth. The parameters obtained from simulations are reported in Table I.

G-L spectral densities (frames (d)-(e) in Figure 1). In Figure 1, the parameter values of ω_{ph} = 20 cm^{-1}, Γ_{hom} = 1 cm^{-1}, Γ_G = 20 cm^{-1} were used with varying Huang-Rhys factors of S = 0.3, 2, and 4. Γ_L = 20 and 60 cm^{-1} were used to simulate symmetric and asymmetric spectral densities, respectively. For small el-ph coupling, the methods produce nearly identical spectra, independent of the shape of the spectral density. However, at larger values of S (>1), the method of Ref. 19 has too much contribution on the low energy side of the PSB and too little contribution on the high energy tail of the PSB. This trend is more evident for asymmetric spectral densities because of the larger Lorentzian width at the high energy side (away from the ZPL).

C. Theoretical fits of the absorption and HB spectra for *Rb.sphaeroides*

Experimental absorption and transient HB spectra for bacterial RCs (5 K) are simulated using the approach outlined in this work with both G-L and lognormal $J(\omega)$. Figure 2 shows fits of experimental spectra for *Rb. sphaeroides* calculated numerically using a G-L spectral density. The calculated absorption matches the experimental curve very well across the entire band. The simulated (red curves) holes (obtained for different burning frequencies and the same parameters as those used in the fit of the P870 band) match the overall shape and width of the experimental HB spectra, but display somewhat larger burning to the high energy side of the hole. The position of this feature is approximately 28 cm^{-1} away from the zero-phonon hole (ZPH), which corresponds to ω_{ph}.

Rb. sphaeroides is used as an example while fits of *Rps. viridis* spectra are not shown for brevity; however, all parameters derived from simulations are given in Table I. Note that for the G-L $J(\omega)$, our parameters are different from those reported previously in Refs. 8, 9, and 28. A comparison of simulations using the sets of parameters from Table I is presented in Figure 3 for *Rb. sphaeroides*. The most significant difference is the Lorentzian width of the phonon spectral density (30 cm^{-1} compared to 55 cm^{-1}).

While previous simulations using the expressions of Hayes *et al.*[19] also provided reasonable fits to the experimental spectra, numerical calculations with these parameters (first row of Table I) result in broadening of the hole width and decreased intensity of the PSB and ω_{sp} holes, as shown in Figure 3. The differences are more pronounced when ω_B is at lower energy than the SDF maximum (frame (a)). When ω_B is at higher energy than ω_{SDF}, the hole shapes are similar for both sets of parameters; although the original parameters derived using the mean-phonon approximation lead to broader spectra due to the improper contribution of multi-phonon modes.

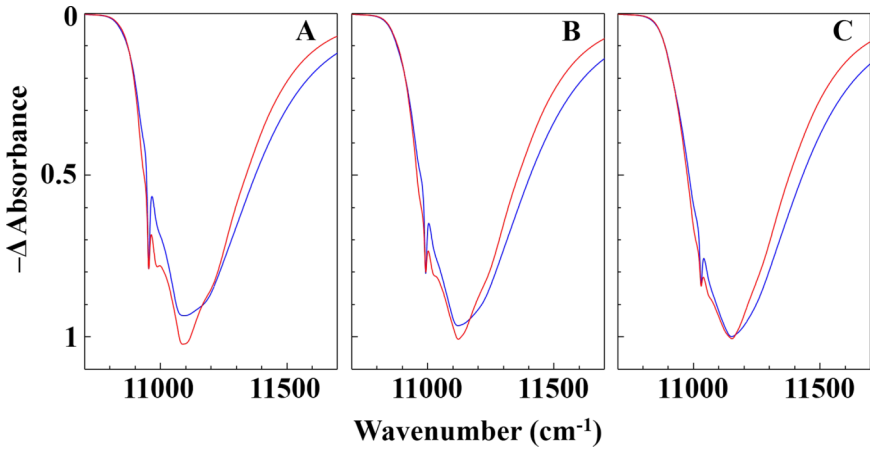

FIG. 3. Simulated transient HB spectra (*Rb. sphaeroides*) calculated with the method outlined in this work. Spectra were simulated using the original (blue curves) and modified parameters (red curves from Figure 2) listed in Table I $\omega_B = 10\,953$, 10 992, and 11 030 cm^{-1} for frames (a)–(c), respectively. Spectra are normalized to ZPH depth.

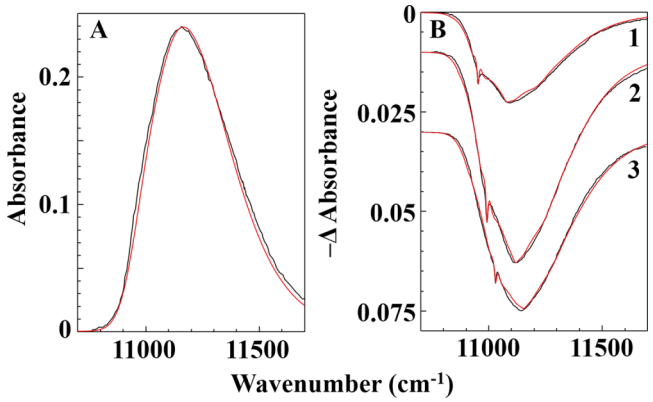

FIG. 4. Experimental data[8] (black curves) from Figure 2 fit with a lognormal $J(\omega)$ (red curves). The parameters obtained from simulations are reported in Table II. Frame (a) is the absorption spectrum and frame (b) shows transient HB spectra with ω_B = 10 953, 10 992, and 11 030 for curves 1–3, respectively.

Figure 4 shows fits of the experimental data[8] assuming a lognormal distribution for $J(\omega)$.[25] While both functional forms of $J(\omega)$ (i.e., G-L and lognormal) fit the experimental data reasonably well, the advantages of the lognormal distribution (see Ref. 25) allow for more physically realistic parameters, including well-defined E_λ, to be elucidated from simulations. The lognormal parameters for *Rb. sphaeroides* and *Rps. viridis* are given in Table II.

IV. CONCLUDING REMARKS

The previous derivation of the lineshape formula using the mean-phonon approximation lead to an equation with improper description of multi-phonon modes, which contribute significantly for systems with strong el-ph coupling, e.g., bacterial RCs. Corrected lineshape expressions are given here, although it is shown that direct numerical evaluation of Eq. (3) (without introducing the mean-phonon approximation) is preferable for calculating absorption and transient HB spectra. Revised el-ph coupling parameters are derived from numerical calculations to replace those found using the mean-phonon approximation. The parameters were obtained from simultaneous fit of transient HB spectra obtained at several burn frequencies as well as the absorption profiles for P870 and P960 bands. Spectra are simulated assuming a lognormal distribution for $J(\omega)$, providing a more physically meaningful representation of el-ph coupling strength in P870 (S_{tot} = 3.2) and P960 (S_{tot} = 3.1) absorption bands for bacterial RCs of *Rb. sphaeroides* and *Rps. viridis*, respectively. The revised values of ω_{sp} (the special pair marker mode) for P960* and P870* are 145 and 125 cm^{-1}, respectively, suggesting that coupled librational motion of the two monomers of the special pair is likely to be a significant contributor to the dynamics.

ACKNOWLEDGMENTS

The authors acknowledge the Division of Chemical Sciences, Geosciences, and Biosciences, Office of Basic Energy Sciences of the U.S. Department of Energy through Grant No. DE-SC0006678 (to R.J.) for support. M.R. thanks the NSF for a Graduate Research Fellowship. This work was initiated by M.R. during his stay at Kansas State University (KSU). T.P. worked on this project at KSU during a summer fellowship supported by NSF and the ASSURE program from the U.S. Department of Defense. Also acknowledged is Dalia Sanchez (KSU) for assistance with spectral fits using the lognormal spectral density function (supported by the Developing Scholars Program).

[1]S. Völker, Annu. Rev. Phys. Chem. **40**, 499 (1989).
[2]R. Jankowiak, M. Reppert, V. Zazubovich, J. Pieper, and T. Reinot, Chem. Rev. **111**, 4546 (2011).
[3]G. S. Schlau-Cohen, A. Ishizaki, and G. R. Fleming, Chem. Phys. **386**, 1 (2011).
[4]K. L. M. Lewis and J. P. Ogilvie, J. Phys. Chem. Lett. **3**, 503 (2012).
[5]P. D. Dahlberg, A. F. Fidler, J. R. Caram, P. D. Long, and G. S. Engel, J. Phys. Chem. Lett. **4**, 3636 (2013).
[6]T. Renger and R. A. Marcus, J. Chem. Phys. **116**, 9997 (2002).
[7]S. G. Johnson, D. Tang, R. Jankowiak, J. M. Hayes, G. J. Small, and D. M. Tiede, J. Phys. Chem. **93**, 5953 (1989).
[8]P. A. Lyle, S. V. Kolaczkowski, and G. J. Small, J. Phys. Chem. **97**, 6924 (1993).
[9]N. R. S. Reddy, S. V. Kolaczkowski, and G. J. Small, J. Phys. Chem. **97**, 6934 (1993).
[10]J. Pieper, J. Voigt, G. Renger, and G. J. Small, Chem. Phys. Lett. **310**, 296 (1999).
[11]S. Matsuzaki, V. Zazubovich, M. Rätsep, J. M. Hayes, and G. J. Small, J. Phys. Chem. B **104**, 9564 (2000).
[12]J. Pieper, R. Schödel, K.-D. Irrgang, J. Voigt, and G. Renger, J. Phys. Chem. B **105**, 7115 (2001).
[13]M. Rätsep and A. Freiberg, Chem. Phys. Lett. **377**, 371 (2003).
[14]K. Riley, R. Jankowiak, M. Rätsep, G. J. Small, and V. Zazubovich, J. Phys. Chem. B **108**, 10346 (2004).
[15]K. Timpmann, M. Rätsep, C. N. Hunter, and A. Freiberg, J. Phys. Chem. B **108**, 10581 (2004).
[16]M. Rätsep and A. Freiberg, J. Lumin. **127**, 251 (2007).
[17]M. Rätsep, J. Pieper, K.-D. Irrgang, and A. Freiberg, J. Phys. Chem. B **112**, 110 (2008).
[18]V. Zazubovich, J. Phys. Chem. B **118**, 13535 (2014).
[19]J. M. Hayes, P. A. Lyle, and G. J. Small, J. Phys. Chem. **98**, 7337 (1994).
[20]J. M. Hayes, J. K. Gillie, D. Tang, and G. J. Small, Biochim. Biophys. Acta **932**, 287 (1988).
[21]B. Neupane, P. Jaschke, R. Saer, J. T. Beatty, M. Reppert, and R. Jankowiak, J. Phys. Chem. B **116**, 3457 (2012).
[22]J. M. Hayes and G. J. Small, J. Phys. Chem. **90**, 4928 (1986).
[23]V. May and O. Kühn, *Charge and Energy Transfer Dynamics in Molecular Systems* (Wiley-VCH, Weinheim, 2000).
[24]E. T. Johnson, V. Nagarajan, V. Zazubovich, K. Riley, G. J. Small, and W. W. Parson, Biochemistry **42**, 13673 (2003).
[25]A. Kell, X. Feng, M. Reppert, and R. Jankowiak, J. Phys. Chem. B **117**, 7317 (2013).
[26]M. Toutounji, J. Chem. Phys. **130**, 094501 (2009).
[27]L. Valkunas, D. Abramavicius, and T. Mančal, *Molecular Excitation Dynamics and Relaxation* (Wiley-VCH, Weinheim, 2013).
[28]S. G. Johnson, D. Tang, R. Jankowiak, J. M. Hayes, G. J. Small, and D. M. Tiede, J. Phys. Chem. **94**, 5849 (1990).